




# RNF152 positively regulates TLR/IL-1R signaling by enhancing MyD88 oligomerization

Mei-Guang Xiong<sup>1,2</sup> , Zhi-Sheng Xu<sup>1</sup>, Yu-Hui Li<sup>1,2</sup>, Su-Yun Wang<sup>1</sup>, Yan-Yi Wang<sup>1,\*</sup>  & Yong Ran<sup>1,\*\*</sup> 

## Abstract

Toll-like receptors (TLRs) are important pattern recognition receptors (PRRs) that are critical for the defense against invading pathogens. IL-1 $\beta$  is an important pro-inflammatory cytokine that also plays pivotal roles in shaping the adaptive immune response. TLRs and interleukin-1 receptor (IL-1R) share similar cytosolic domains and signaling processes. In this study, we identify the E3 ubiquitin ligase RNF152 as a positive regulator of TLR/IL-1R-mediated signaling. Overexpression of RNF152 potentiates IL-1 $\beta$ - and LPS-induced NF- $\kappa$ B activation in an ubiquitination-independent manner, whereas knockdown of RNF152 has the opposite effects. RNF152-deficient mice produce less inflammatory cytokines in response to LPS and are more resistant to LPS-induced lethal endotoxemia. Mechanistically, RNF152 interacts with the adaptor protein MyD88 and enhances oligomerization of MyD88, which is essential for the recruitment of downstream signaling components and activation of TLR/IL-1R-mediated signal transduction. Our findings suggest that RNF152-mediated oligomerization of MyD88 is important for TLR/IL-1R-mediated inflammatory response.

**Keywords** IL-1 $\beta$ ; LPS; MyD88; RNF152; toll-like receptor

**Subject Categories** Immunology; Post-translational Modifications & Proteolysis; Signal Transduction

**DOI** 10.15252/embr.201948860 | Received 11 July 2019 | Revised 16 December 2019 | Accepted 19 December 2019 | Published online 13 January 2020

**EMBO Reports (2020) 21: e48860**

## Introduction

The innate immune system senses invading pathogens by germline-encoded pattern recognition receptors (PRRs) which recognize specific molecular patterns of pathogens. One important class of PRRs is TLRs. Members of TLRs recognize various microbial components such as nucleic acids, lipids, proteins, lipoproteins, and glycoproteins, leading to the activation of innate immune response as well as production of pro-inflammatory cytokines [1,2]. IL-1 $\beta$  is an important pro-inflammatory cytokine which could be induced by

PRR-mediated signaling. It is critical for both local and systemic inflammation and contributes to both innate and adaptive immune responses [3]. IL-1 $\beta$  binds to the IL-1 receptor (IL-1R) to initiate signal transduction. TLRs and IL-1R share a common toll/interleukin-1 receptor (TIR) domain in their intracellular region [1]. Upon ligand binding, all TLRs except TLR3 and IL-1R recruit the same adaptor protein myeloid differentiation factor 88 (MyD88) to the receptors [4,5]. MyD88 subsequently recruits several kinases, including IL-1 receptor-associated kinase 1 (IRAK1), IRAK2, and IRAK4, as well as E3 ubiquitin ligase tumor necrosis factor receptor-associated factor 6 (TRAF6) to form a protein complex termed Myddosome [5–7]. TRAF6 possesses an E3 ubiquitin ligase activity that catalyzes K63-linked autoubiquitination and/or the synthesis of free K63-linked polyubiquitin chains. The K63-linked polyubiquitin chains further recruit the ubiquitin-binding TAK1-TAB 1/2/3 complex, resulting in the activation of TAK1 [8,9]. Activated TAK1 then phosphorylates IKK $\beta$  and mitogen-activated protein kinase kinases, leading to the induction of pro-inflammatory cytokines and chemokines.

The activation of TLR/IL-R signaling is delicately regulated by the host to prevent autoimmune diseases, inflammatory disorders, and cancer. For example, it has been reported that the activation of MyD88 is tightly regulated. MyD88 is comprised of an N-terminal death domain (DD), an intermediate domain (ID), and a C-terminal TIR domain. Under normal physiological status, MyD88 is kept in an autoinhibited state by intramolecular interaction between the TIR domain and DD. Upon stimulation, MyD88 is recruited to the receptor via TIR-TIR interactions, which in turn releases the DD of MyD88 and consequently initiates its oligomerization [10]. Although intensive efforts have been made to characterize the signaling mediated by TLR/IL-1R [11–17], the regulation of MyD88 oligomerization is still enigmatic.

Ring finger protein 152 (RNF152) is an E3 ubiquitin ligase with a RING domain and a transmembrane (TM) domain. Previous studies have suggested that RNF152 promotes apoptosis [18] and negatively regulates mTORC1 signaling by mediating K63-linked polyubiquitination of RagA [19]. In this study, we demonstrate that RNF152 positively regulates TLR/IL-1R-mediated inflammatory response by facilitating oligomerization of MyD88, which subsequently promotes

1 Key Laboratory of Special Pathogens and Biosafety, Wuhan Institute of Virology, Center for Biosafety Mega-Science, Chinese Academy of Sciences, Wuhan, China

2 University of Chinese Academy of Sciences, Beijing, China

\*Corresponding author. Tel: +86 027 87198095; E-mail: wangyy@wh.iov.cn

\*\*Corresponding author. Tel: +86 027 87198026; E-mail: ranyong@wh.iov.cn

the assembly of Myddosome. Our study suggests that RNF152 is essential for TLR/IL-1R-mediated, MyD88-dependent signal transduction.

## Results and Discussion

### Identification of RNF152 as a positive regulator of IL-1 $\beta$ -triggered signaling

Due to the importance of IL-1 $\beta$  in inflammatory response, we attempted to identify proteins that regulate IL-1 $\beta$  signaling by screening ~ 16,000 independent human cDNA expression clones for their abilities to regulate IL-1 $\beta$ -triggered activation of NF- $\kappa$ B by reporter assays. This effort led to identification of RNF152 as a candidate regulator of IL-1 $\beta$  signaling (Fig EV1A and B, and Dataset EV1). In this screening, multiple proteins that have been reported to be involved in IL-1 signaling were also identified, indicating that the experimental system is effective and reliable. As shown in Fig 1A, overexpression of RNF152 activated NF- $\kappa$ B reporter in a dose-dependent manner and potentiated IL-1 $\beta$ -triggered NF- $\kappa$ B activation. Consistently, overexpression of RNF152 enhanced IL-1 $\beta$ -induced transcription of inflammatory cytokines such as *IL8*, *CXCL1*, and *CXCL10* (Fig 1B). However, overexpression of RNF152 showed little effects on NF- $\kappa$ B activation induced by SeV, which is mediated through the RIG-I-VISA signaling pathway (Fig 1C).

### RNF152 is involved in IL-1R/TLR4-mediated signaling

To determine whether endogenous RNF152 regulates IL-1 $\beta$ -triggered signaling, we designed three RNF152-siRNAs which down-regulated the transcription of RNF152 to different levels (Fig 1D). Reporter assays indicated that knockdown of RNF152 inhibited IL-1 $\beta$ -induced activation of NF- $\kappa$ B (Fig 1E). The degrees of inhibition were correlated with the efficiencies of RNF152 knockdown by these siRNAs (Fig 1D and E). Since the signal

transduction downstream of IL-1R and TLR4 is similar, we wondered whether RNF152 is also involved in TLR4-initiated signaling. Stimulation of cells with the TLR4 ligand LPS revealed that knockdown of RNF152 also inhibited TLR4-mediated NF- $\kappa$ B activation (Fig 1F). Consistent with these observations, knockdown of RNF152 resulted in impaired transcription of *IL1B*, *IL6*, and *IL8* genes in response to IL-1 $\beta$  and LPS treatment in human foreskin fibroblasts (HFFs) and human peripheral blood mononuclear cells (PBMCs; Fig 1G and H). Knockdown of RNF152 also impaired the phosphorylation of IKK $\alpha$ / $\beta$  and p38 triggered by IL-1 $\beta$  and LPS, which are key indicators of activation of these kinases (Fig 1I). Interestingly, the mRNA level of RNF152 was up-regulated in HFFs after LPS stimulation (Fig EV1C). Taken together, these results suggest that endogenous RNF152 is involved in IL-1R/TLR4-mediated signaling.

### RNF152 positively regulates TLR/IL-1R-mediated inflammatory responses *in vivo*

To further investigate the function of RNF152 *in vivo*, we utilized *Rnf152* knockout mice which were described previously [19]. RNF152 deficiency showed little effects on the composition of T cells, B cells, and NK cells in thymus and spleen, indicating that RNF152 has no effects on the development of these cells (Fig EV2). We prepared several types of primary murine cells including mouse embryo fibroblasts (MEFs), bone marrow-derived macrophages (BMDMs), and bone marrow-derived dendritic cells (BMDCs) from wild-type and *Rnf152*<sup>-/-</sup> mice and stimulated these cells with IL-1 $\beta$ , LPS, PGN (a ligand for TLR2), poly(I:C) (a ligand for TLR3), SeV, and HSV-1, and then examined the transcription of pro-inflammatory genes including *Il1b*, *Il6*, *Cxcl10*, *Tnfa*, and *Ifnb1*. We found that RNF152 deficiency impaired IL-1 $\beta$ -, LPS-, and PGN-induced but not poly(I:C)-induced transcription of *Il1b*, *Il6*, and *Cxcl10* in MEFs (Fig 2A), indicating that RNF152 is required for IL-1R-, TLR2-, and TLR4- but not TLR3-mediated signaling. Interestingly, LPS-induced transcription of *Ifnb1*, which is mediated by the TLR4-TRIF axis, was not affected by RNF152

**Figure 1. Identification of RNF152 as a positive regulator of TLR/IL-1R-mediated signaling.**

- A Effects of RNF152 on IL-1 $\beta$ -induced NF- $\kappa$ B activation. HEK293T cells were transfected with pNifty-Luciferase reporter (1 ng) and RNF152 plasmids as indicated. Twenty-four hours later, these cells were stimulated with IL-1 $\beta$  (20 ng/ml) or left untreated for 10 h before luciferase assays were performed. The pNifty-Luciferase reporter plasmid (InvivoGen) contains five NF- $\kappa$ B binding sites. Data were analyzed by one-way ANOVA, followed by the Dunnett *post hoc* test.
- B Effects of RNF152 on IL-1 $\beta$ -induced transcription of inflammatory cytokine genes. HEK293T cells were transfected with RNF152 plasmid (200 ng). Twenty-four hours later, cells were left untreated or stimulated with IL-1 $\beta$  for 2 h before RT-qPCR assay. Data were analyzed by unpaired, two-tailed Student's *t*-test.
- C Effects of RNF152 on SeV-induced NF- $\kappa$ B promoter activation. The experiments were similarly performed as in (A), except that cells were infected with SeV for 10 h.
- D Knockdown efficiency of RNF152 siRNA. HEK293T cells were transfected with RNF152 plasmid (200 ng) and the indicated siRNAs (final concentration, 40 nM).
- E, F Effects of RNF152 knockdown on IL-1 $\beta$ - and LPS-induced NF- $\kappa$ B activation. HEK293T cells were transfected with Nifty reporter and the indicated siRNAs (final concentration, 40 nM). Forty-eight hours later, cells were left untreated or stimulated as indicated for 10 h. As for LPS stimulation (50 ng/ml), additional plasmids of TLR4 (1.5 ng) and MD2 (2.5 ng) were transfected (F). The knockdown efficiency was confirmed by RT-qPCR assay. TLR4 was constructed into pMSCV without tag. MD2 was constructed into pLX304 with a V5 tag in its C-terminus. Data were analyzed by one-way ANOVA, followed by the Dunnett *post hoc* test.
- G, H qPCR analysis of mRNA levels of the indicated genes. HFFs and PBMCs were transfected with the negative control (NC) or 2# siRNA (final concentration, 40 nM). Forty-eight hours later, cells were left untreated or stimulated with IL-1 $\beta$  (20 ng/ml) for 2 h or stimulated with LPS (50 ng/ml) for 4 h. Data were analyzed by unpaired, two-tailed Student's *t*-test.
- I Immunoblot analysis of the indicated proteins in RNF152 knockdown HFFs. HFFs were transfected with NC or 2# siRNA. Forty-eight hours later, cells were left untreated or stimulated with IL-1 $\beta$  (20 ng/ml) or LPS (50 ng/ml) as indicated.

Data information: Data of (A–C, E–H) are representative of three independent experiments with similar results. Graphs show mean  $\pm$  SD, three biological repeats, \**P* < 0.05, \*\**P* < 0.01, \*\*\**P* < 0.001. Data of (D, I) are representative of three independent experiments. Source data are available online for this figure.

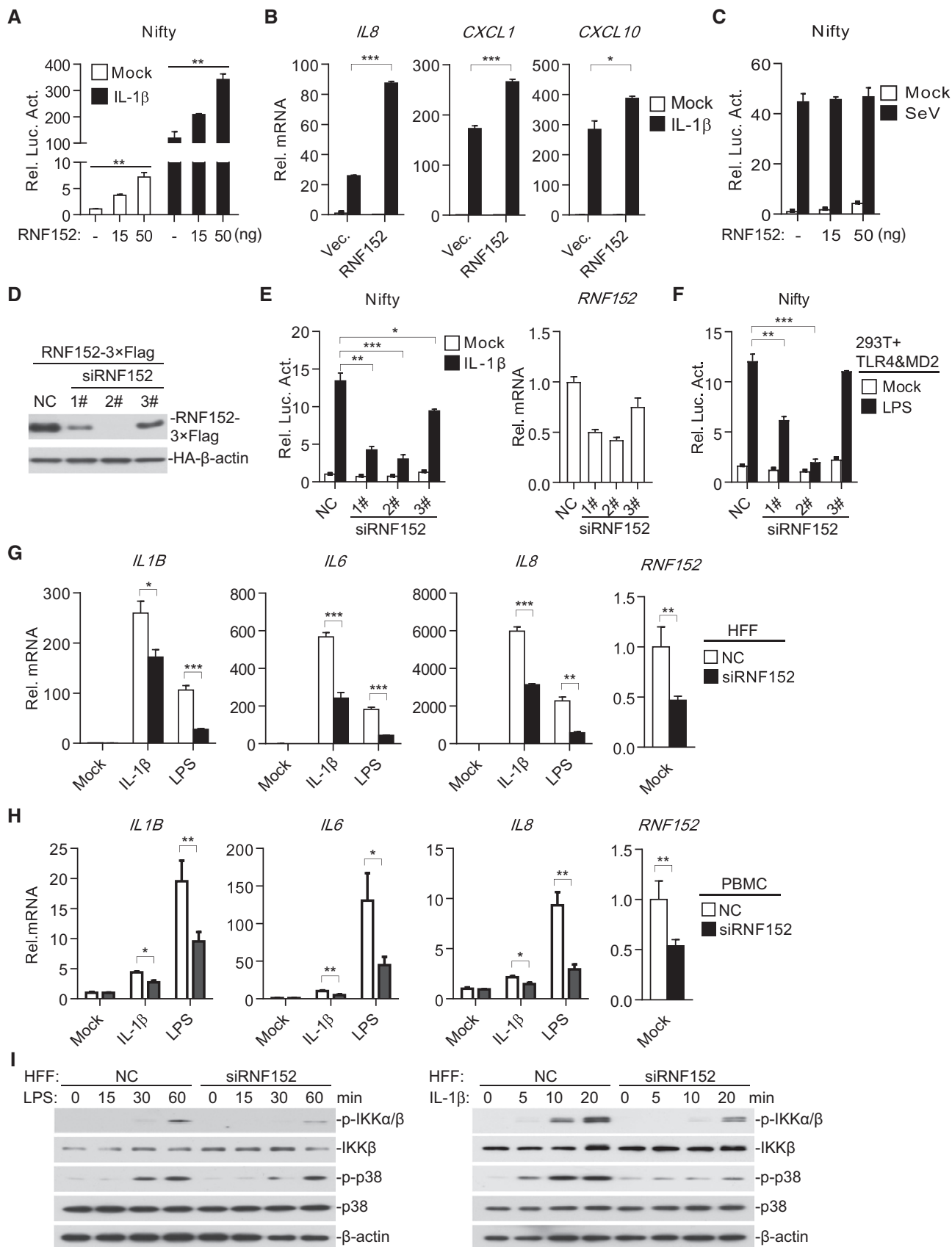


Figure 1.

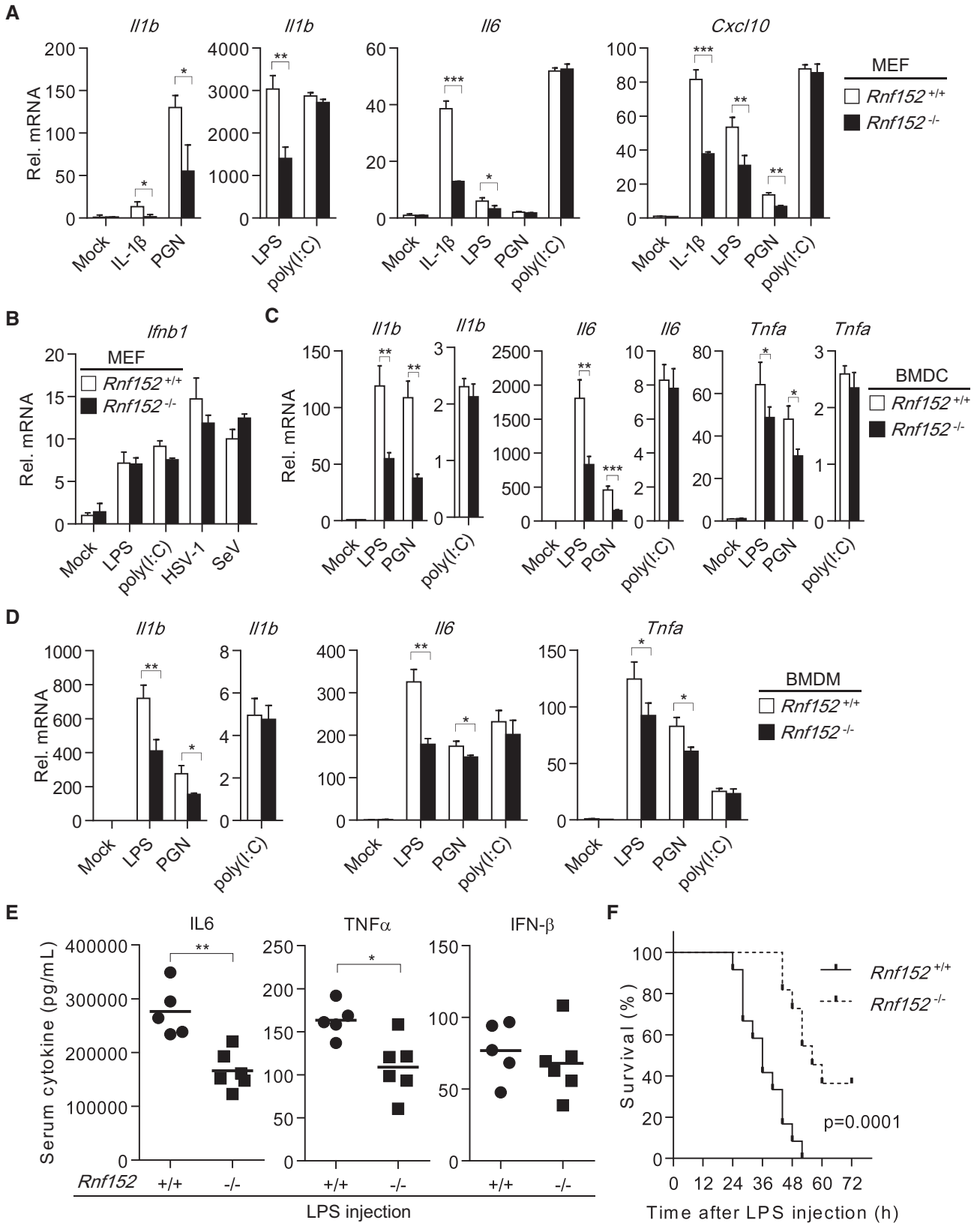


Figure 2.

**Figure 2. RNF152 deficiency impairs TLR/IL-1R-mediated signaling.**

- A–D qPCR analysis of mRNA levels of the indicated genes. MEFs (A, B), BMDCs (C), and BMDMs (D) from *Rnf152*<sup>+/+</sup> or *Rnf152*<sup>-/-</sup> mice were left untreated or stimulated with IL-1 $\beta$  (50 ng/ml), PGN (a ligand for TLR2, 10  $\mu$ g/ml), poly(I:C) (a ligand for TLR3, 10  $\mu$ g/ml), or LPS (a ligand for TLR4, 50 ng/ml) for 2 h, or infected with HSV-1 or SeV for 6 h as indicated before RNA extraction. Data were analyzed by unpaired, two-tailed Student's *t*-test.
- E Effects of RNF152 deficiency on LPS-induced cytokine production. Age- and sex-matched *Rnf152*<sup>+/+</sup> or *Rnf152*<sup>-/-</sup> mice were intraperitoneally injected with LPS (10 mg/kg) for 3 h, and the concentrations of IL-6, TNF $\alpha$ , and IFN- $\beta$  in the sera were determined by ELISA. Data were analyzed by unpaired, two-tailed Student's *t*-test.
- F Effects of RNF152 deficiency on LPS-induced inflammatory death of mice. Age- and sex-matched *Rnf152*<sup>+/+</sup> (*n* = 12) or *Rnf152*<sup>-/-</sup> (*n* = 11) mice were intraperitoneally injected with LPS (10 mg/kg). The survival of mice was monitored every 4 h. The log-rank (Mantel–Cox) test was applied to analyze the statistical significance.

Data information: Data of (A–D) are representative of three independent experiments. Graphs show mean  $\pm$  SD; three biological repeats. \**P* < 0.05, \*\**P* < 0.01, \*\*\**P* < 0.001.

deficiency (Fig 2B), suggesting RNF152 specifically regulates MyD88- but not TRIF-mediated signaling. In addition, SeV- and HSV-1-induced transcription of *Ifnb1*, which is dependent on the RIG-I-VISA and cGAS-STING signaling, respectively, was not affected by RNF152 deficiency (Fig 2B). Consistently, similar results were also obtained with BMDCs and BMDMs (Fig 2C and D). These results together suggest that RNF152 specifically regulates TLR/IL-1R-mediated, MyD88-dependent signaling.

Next, we evaluated the roles of RNF152 in LPS-induced inflammatory response *in vivo*. The results showed that LPS-induced production of IL-6 and TNF $\alpha$  was significantly decreased in the sera of RNF152-deficient mice compared to wild-type mice (Fig 2E). However, RNF152 deficiency had no obvious effects on LPS-induced IFN- $\beta$  production (Fig 2E), which is mediated by TRIF-dependent signaling as described above. These results further confirmed the conclusion that RNF152 is required for MyD88-dependent but not TRIF-dependent signaling pathways. In the LPS-induced endotoxemia model, inflammatory cytokines induced after LPS administration are major contributors to lethal endotoxemia. Consistent with a lower level of inflammatory cytokines production, RNF152-deficient mice displayed later onset of death and a lower percentage of lethality in comparison with their wild-type counterparts after the LPS challenge (Fig 2F). Taken together, these data suggest that RNF152 is an important positive regulator of TLR/IL-1R-mediated inflammatory responses *in vivo*.

**Membrane association but not the E3 ligase activity of RNF152 is required for its regulation of TLR/IL-1R-mediated signaling**

Ring finger protein 152 is an E3 ubiquitin ligase which mediates autoubiquitination and mediates ubiquitination of the RagA GTPase in response to amino acid starvation [18,19]. We next investigated whether the E3 ubiquitin ligase activity of RNF152 is required for the regulation of TLR/IL-1R-mediated signaling. We constructed an E3-deficient point mutation of RNF152 (RNF152-C30S) and a truncation of RNF152 which lacks the RING domain (RNF152- $\Delta$ R). As shown in Fig EV3A, compared with wild-type RNF152, autoubiquitination of these mutants decreased markedly, indicating the E3 ubiquitin ligase activity is abrogated. Intriguingly, these E3-deficient mutants of RNF152 still potentiated IL-1 $\beta$ -stimulated NF- $\kappa$ B activation, suggesting the enzymatic activity of RNF152 is not required (Fig 3A).

Since RNF152 contains a TM domain, we further examined the role of it in the regulation of TLR/IL-1R signaling. Confocal microscopy indicated that RNF152 partially co-localized with early endosomes, late endosomes, and lysosomes (Fig EV3B), and such localization is dependent on its TM domain [19]. Notably, deletion of the TM domain deprived the ability of RNF152 to potentiate IL-1 $\beta$ -stimulated NF- $\kappa$ B activation (Fig. 3A), suggesting the membrane localization of RNF152 is important for its function in TLR/IL-1R-mediated signaling.

**Figure 3. RNF152 is associated with components of Myddosome.**

- A The effects of RNF152 and its mutants on IL-1 $\beta$ -induced NF- $\kappa$ B activation. The plasmids of RNF152 and its mutants were transfected into HEK293T cells to perform reporter luciferase assay. The expression of RNF152 and its mutants was shown at the bottom.  $\Delta$ R indicates the deletion of the RING finger domain of RNF152, and  $\Delta$ TM indicates the deletion of the transmembrane domain of RNF152. Data were analyzed by one-way ANOVA, followed by the Dunnett *post hoc* test.
- B RNF152 interacted with components of Myddosome. HEK293T cells were transfected with the indicated plasmids. Twenty-four hours later, cells were subjected to co-immunoprecipitation and immunoblot with the indicated antibodies. IRAK1-KD indicates kinase-dead mutant of IRAK1 (K239A); IRAK4-KD indicates kinase-dead mutant of IRAK4 (K213/214A).
- C HEK293T cells were transfected with the indicated plasmids. Twenty-four hours later, cell lysates were subjected to pull-down assay with *in vitro* purified and GST-tagged RNF152- $\Delta$ TM.
- D Prokaryotic expressed and purified RNF152- $\Delta$ TM, MyD88, and TRAF6 were subjected to *in vitro* pull-down assay. The asterisk indicates a non-specific band.
- E Domain mapping of RNF152-MyD88 interaction. The upper panels show schematic representations of MyD88. HEK293T cells were transfected with the indicated plasmids and were subjected to co-immunoprecipitation and immunoblot with the indicated antibodies.
- F Immortalized MEFs stably transduced with RNF152-3 $\times$ Flag were stimulated with IL-1 $\beta$  (50 ng/ml) or LPS (50 ng/ml) for the indicated times before subjected to co-immunoprecipitation and immunoblot with the indicated antibodies. The asterisk indicates a non-specific band.
- G Mouse lung fibroblast cells (MLFs) from *Myd88*<sup>+/+</sup> and *Myd88*<sup>-/-</sup> mice were transfected with plasmids of pNifty-Luciferase reporter (20 ng) and vector or RNF152 (400 ng) as indicated. Twenty-four hours later, luciferase assays were performed. Data were analyzed by unpaired, two-tailed Student's *t*-test.

Data information: Data of (A and G) are representative of three independent experiments. Graphs show mean  $\pm$  SD; three biological repeats. \**P* < 0.05, \*\**P* < 0.01, \*\*\**P* < 0.001.

Source data are available online for this figure.

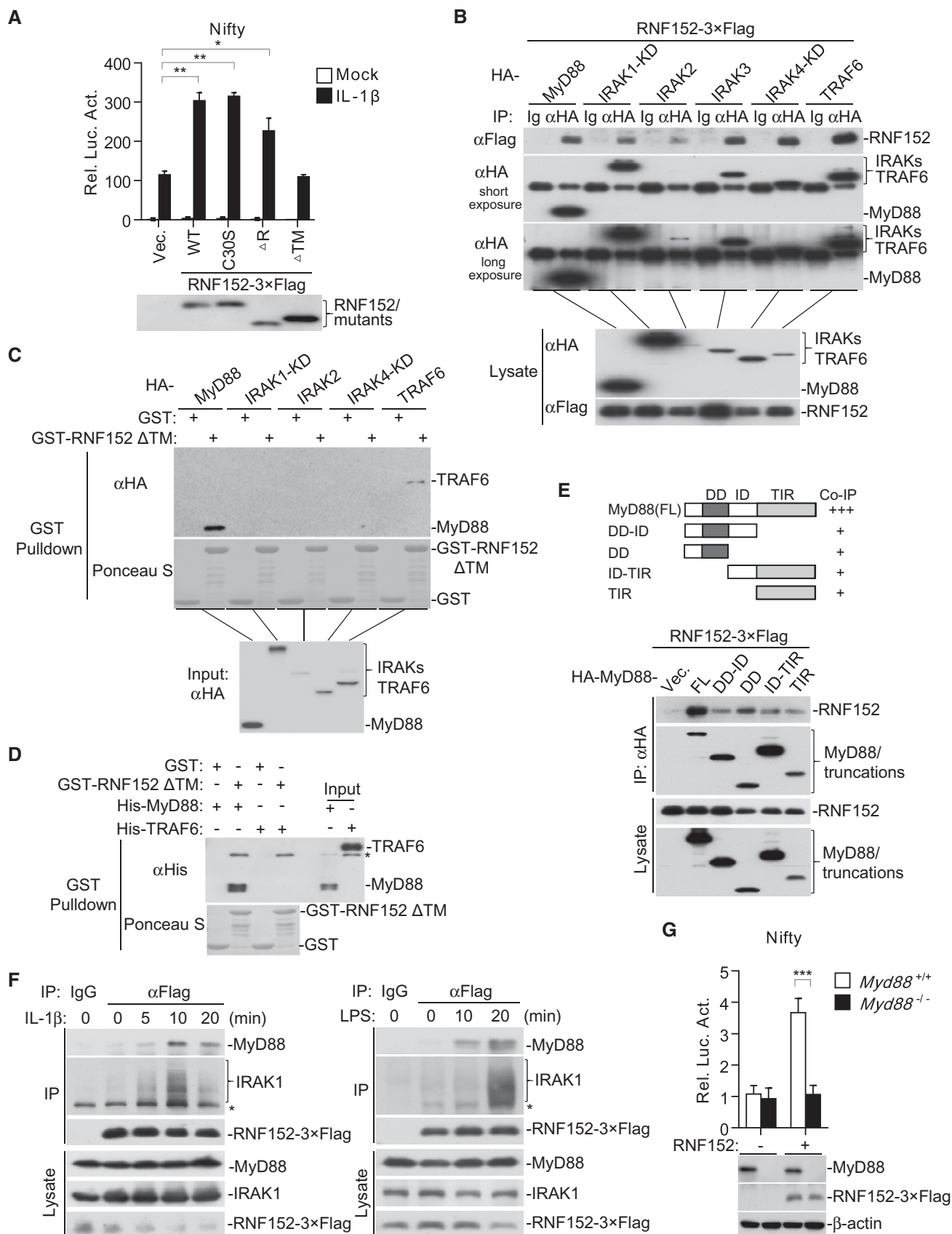


Figure 3.

### RNF152 associates with MyD88

We next tried to elucidate the mechanism by which RNF152 regulates TLR/IL-1R signaling. In co-immunoprecipitation experiments, we found that RNF152 was associated with MyD88, IRAK1-KD, IRAK2, IRAK3, IRAK4-KD, and TRAF6 (Fig 3B), all of which are components of the Myddosome [20]. To prevent proteasome-mediated RNF152 degradation triggered by co-transfection with wild-type IRAK1 and IRAK4 (Fig EV4A and B), we used kinase-inactive mutants IRAK1-KD and IRAK4-KD in these experiments. In similar co-immunoprecipitations, RNF152 was not associated with IKK $\alpha$  and IKK $\beta$ , components downstream of the Myddosome (Fig EV4C). In addition, *in vitro* pull-down assay using purified recombinant RNF152- $\Delta$ TM, a truncation which lacks the TM domain, and cell lysates transfected with MyD88, TRAF6, or the indicated IRAKs showed that RNF152- $\Delta$ TM bound to MyD88, TRAF6 but not IRAKs (Fig 3C). However, further pull-down assays using prokaryotic expressed RNF152- $\Delta$ TM, MyD88, and TRAF6 showed that RNF152 directly interacted with MyD88 but not TRAF6 (Fig 3D). The difference of RNF152-TRAF6 interaction observed in Fig 3C and D is probably caused by indirect interaction between RNF152 and TRAF6-interacting proteins in cells transfected with TRAF6. Moreover, we found that both the DD and TIR domain of MyD88 interacted with RNF152, although to a lower extent than the full-length MyD88 (Fig 3E). To confirm the interaction between RNF152 and MyD88 endogenously, we established immortalized MEFs stably expressing RNF152-3 $\times$ Flag. After IL-1 $\beta$  and LPS stimulation, endogenous MyD88 and IRAK1 interacted with RNF152 (Fig 3F). Furthermore, overexpression of RNF152 failed to activate NF- $\kappa$ B activation in MyD88-deficient mouse lung fibroblasts (MLFs), suggesting that RNF152 functions in a MyD88-dependent manner (Fig 3G).

Although RNF152 is an E3 ubiquitin ligase, the effects of RNF152 in TLR/IL-1R-mediated signaling are not dependent on its E3

ubiquitin ligase activity (Fig 3A). Consistently, RNF152 showed no effects on the turnover of IL1R1 and TLR4 (Fig EV4D and E) or the ubiquitination of Myddosome components (Fig EV4F). Taken together, these results suggest that RNF152 associates with Myddosome through directly binding to MyD88.

### RNF152 enhances the oligomerization of MyD88

Oligomerization of MyD88 is a pivotal step in its activation and in TLR/IL-1R-mediated signaling [21–24]. The crystal structure of the MyD88: IRAK4: IRAK2 DD complex suggests that this complex consists of six MyD88 DD [25]. In addition, another study suggests that MyD88 oligomerization is mediated by low affinity intermolecular interactions between the DDs, making the process reversible [22]. However, how MyD88 oligomerization is stabilized and regulated remains unclear.

Confocal microscopy showed that MyD88 was dispersed through the cytosol and barely co-localized with RNF152 under normal physiological condition (Fig 4A). After stimulation with IL-1 $\beta$  and LPS, MyD88 aggregated to form puncta structures, where it strongly co-localized with RNF152 (Fig 4A). It is highly possible that the MyD88 puncta is an indication of its oligomerization, since MyD88 forms oligomer after activation as described above. Co-immunoprecipitation experiments showed that RNF152 markedly enhanced the interaction of Flag-tagged and HA-tagged MyD88 in a dose-dependent manner (Fig 4B). *In vitro* binding assay further confirmed that RNF152 could promote the self-association of MyD88 (Fig 4C). Notably, although the GST-RNF152- $\Delta$ TM bound to MyD88 and promoted its self-association *in vitro* (Fig 4C), RNF152- $\Delta$ TM lost the ability to enhance the self-association of MyD88 in cells (Fig 4D), suggesting that membrane association is required for RNF152 to facilitate MyD88 oligomerization. In contrast, RNF152-C30S and RNF152- $\Delta$ R enhanced dimerization or oligomerization of MyD88 similarly as RNF152-WT (Fig 4D),

#### Figure 4. RNF152 enhances the oligomerization of MyD88.

- A Analysis of the co-localization of MyD88 with RNF152 by confocal microscopy. MEFs stably transduced with RNF152-3 $\times$ Flag were stimulated with IL-1 $\beta$  (20 ng/ml) or LPS (50 ng/ml) for the indicated times, and were stained with anti-MyD88 antibody (diluted to 10  $\mu$ g/ml, green) and anti-Flag antibody (diluted to 10  $\mu$ g/ml, red). Nuclei were stained with DAPI (blue). Representative images were shown. The arrows indicate co-localized puncta of MyD88 and RNF152. The specificity of the anti-MyD88 antibody was tested (Fig EV5A and B).
- B Effects of RNF152 on the oligomerization of MyD88. HEK293T cells were transfected with the indicated plasmids, and then, co-immunoprecipitation and immunoblot analysis were performed.
- C The lysates of HEK293T cells transfected with HA-MyD88 (2  $\mu$ g) and purified His-tagged MyD88 were mixed together with purified RNF152- $\Delta$ TM or GST, and then subjected to co-immunoprecipitation with anti-His antibody.
- D Effects of RNF152 and its mutants on the oligomerization of MyD88. HEK293T cells were transfected with the indicated plasmids, and then, co-immunoprecipitation and immunoblot analysis were performed.
- E Effects of overexpression of RNF152 on the oligomerization of MyD88. HEK293T cells were transfected with HA-MyD88 (2  $\mu$ g) and RNF152-3 $\times$ Flag (WT) or its mutants (C30S/ $\Delta$ R/ $\Delta$ TM) plasmids (1.5  $\mu$ g). Twenty-four hours later, cells were collected and lysed, followed by gel filtration. Fraction size was calibrated with the gel filtration standard (Bio-Rad 151-1901).
- F Effects of RNF152 knockdown on the oligomerization of MyD88. HEK293T cells were transfected with the indicated siRNA. Thirty hours later, cells were re-transfected with HA-tagged and Flag-tagged MyD88 plasmids, and then, co-immunoprecipitation and immunoblot analysis were performed. The knockdown efficiency was confirmed and shown in Fig EV5C.
- G Effects of RNF152 on the oligomerization of endogenous MyD88. RAW 264.7 cells were transfected with siRNA targeting mouse Rnf152 (final concentration, 40 nM) or NC. Forty-eight hours later, cells were collected and stimulated with LPS (1  $\mu$ g/ml) for 5 min and then were lysed, followed by gel filtration. Fraction size was calibrated with the gel filtration standard (Bio-Rad 151-1901). The knockdown efficiency was confirmed and shown in Fig EV5D.
- H BMDMs prepared from *Rnf152*<sup>+/+</sup> and *Rnf152*<sup>-/-</sup> mice were stimulated with LPS (50 ng/ml) for the indicated times before subjected to co-immunoprecipitation and immunoblot with the indicated antibodies. The asterisk indicates a non-specific band.

Data information: Data of (B–H) are representative of two to three independent experiments.

Source data are available online for this figure.

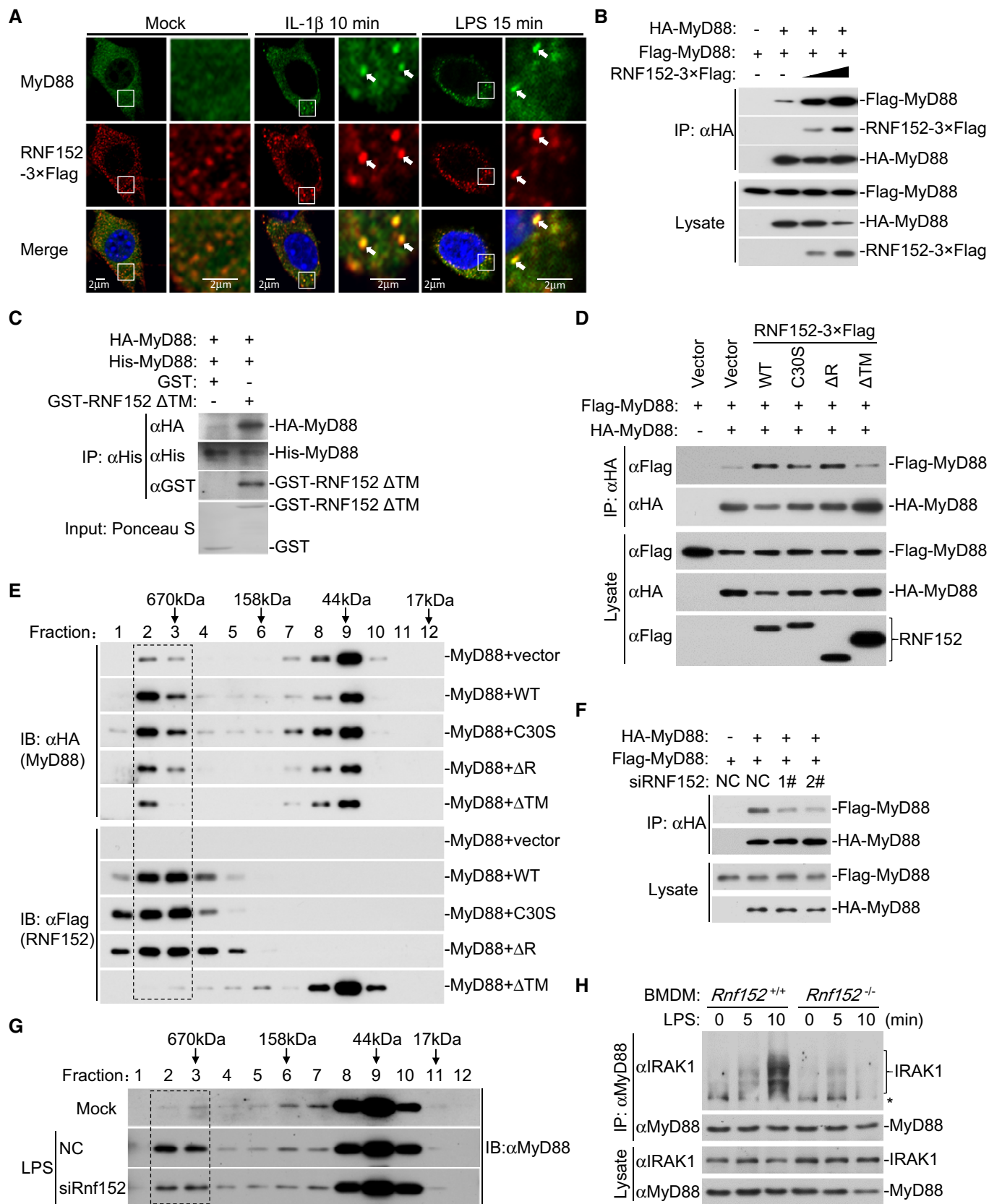
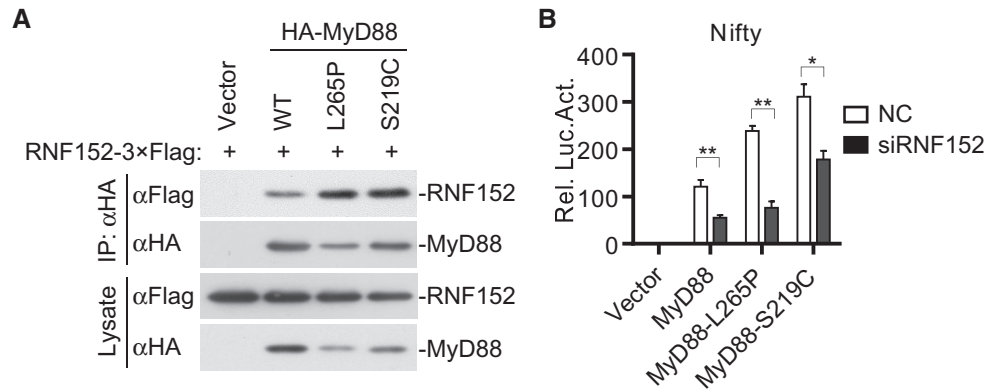


Figure 4.





**Figure 5. RNF152 is involved in the NF- $\kappa$ B activation mediated by lymphoma-associated mutants of MyD88.**

**A** RNF152 interacts with lymphoma-associated mutants of MyD88. HEK293T cells were transfected with the indicated plasmids. Twenty-four hours later, cells were subjected to co-immunoprecipitation and immunoblot with the indicated antibodies. L265P and S219C are representatives of B-cell lymphoma-associated mutants of MyD88. Data are representative of three independent experiments.

**B** The effects of RNF152 knockdown on MyD88- and its mutant-mediated NF- $\kappa$ B activation. HEK293T cells were transfected with NC or 2# siRNA. Forty hours later, cells were transfected with plasmids of pNifty-Luciferase reporter (5 ng) and MyD88 mutants as indicated. Twenty-four hours later, luciferase assays were performed. Data were analyzed by unpaired, two-tailed Student's *t*-test. Data are representative of three independent experiments. Graphs show mean  $\pm$  SD, three biological repeats, \**P* < 0.05, \*\**P* < 0.01.

Source data are available online for this figure.

indicating that the E3 ubiquitin ligase activity is not required in this process.

Next, we performed gel filtration experiments to examine the oligomerization of MyD88 more directly. A small portion of MyD88 was eluted in the high-molecular weight fractions, which represents the oligomerized MyD88. Overexpression of RNF152-WT, RNF152-C30S, RNF152- $\Delta$ R but not RNF152- $\Delta$ TM increased distribution of MyD88 to the high-molecular weight fractions (Fig 4E). Interestingly, majorities of RNF152-WT/C30S/ $\Delta$ R but not RNF152- $\Delta$ TM were also eluted in the high-molecular weight fractions (Fig 4E, lower panels), indicating that membrane-associated RNF152 can form "ordered" oligomers, which may act as scaffolds to promote the oligomerization of MyD88. Conversely, knockdown of RNF152 impaired self-association of MyD88 (Figs 4F and EV5C). After stimulation with LPS, a portion of endogenous MyD88 was eluted in the high-molecular weight fractions (Fig 4G, middle panel, dashed box). However, knockdown of RNF152 decreased the ratio of MyD88 distributed in the high-molecular weight fractions, indicating that RNF152 is important for the oligomerization of MyD88 (Fig 4G, bottom panel, and Fig EV5D). Since oligomerization of MyD88 is essential for the recruitment of IRAKs, LPS-induced recruitment of IRAK1 to MyD88 was also impaired by RNF152 deficiency (Fig 4H). Collectively, these results suggest that RNF152 is essential for MyD88 oligomerization and downstream signal transduction. It has been reported that lymphoma-associated mutations, particularly Leu265Pro (L265P), in the MyD88 TIR domain cause the constitutive activation of NF- $\kappa$ B due to spontaneous oligomerization of MyD88 [24,26]. Therefore, we further examined whether RNF152 is involved in these mutant-mediated NF- $\kappa$ B activations. We found that RNF152 interacted with MyD88-L265P and MyD88-S219C more strongly than with the MyD88-WT (Fig 5A). Furthermore, these MyD88 mutant-mediated NF- $\kappa$ B activations were impaired in RNF152 knockdown

cells (Fig 5B), indicating that RNF152 plays an important role in these lymphoma-associated mutant-mediated signaling. These observations suggest a possible role of RNF152 in MyD88-relevant B-cell lymphomas.

In this study, we identified RNF152 as a positive regulator of TLR/IL-1R-mediated signaling. The oligomerization of MyD88 and assembly of Myddosome have been established by several studies [10,22–25]. We further found that RNF152 promotes MyD88 activation and Myddosome formation by interacting with MyD88 and facilitating MyD88 oligomerization. These findings have provided new mechanistic insights into MyD88-mediated signal transduction. Previous studies suggest that both the DD and TIR of MyD88 could mediate its dimerization and oligomerization [25,27]. In this study, we found that the membrane-localized RNF152 interacts with both the DD and TIR of MyD88, which probably provide additional links between two or more MyD88 molecules, therefore enhancing the oligomerization of MyD88. Further exploration of how RNF152 facilitates the oligomerization of MyD88 by more sensitive and direct techniques, such as crystallography, would provide more details. In addition, how the membrane localization of RNF152 affects its function in the regulation of TLR/IL-1R-mediated signaling remains to be clarified. Given the pivotal roles of MyD88 in immune defense and inflammatory response, it will be interesting to investigate the roles of RNF152 in MyD88-relevant pathogenesis, such as B-cell lymphomas.

## Materials and Methods

### Reagents and antibodies

Recombinant human IL-1 $\beta$  (Peprotech), peptidoglycan (PGN; Sigma), LPS (Sigma), and SYBR (Bio-Rad) were purchased from the

indicated companies. Monoclonal anti-Flag M2 antibody and monoclonal anti-Flag M2-Peroxidase (HRP) antibody (Sigma-Aldrich, 1:1,000); antibodies against HA (OriGene, 1:2,000), myc (ABclonal, 1:2,000),  $\beta$ -actin (ABclonal, 1:10,000), phospho-IKK $\alpha$  (Ser176)/IKK $\beta$  (Ser177; C84E11; Cell Signaling Technology, 1:500), IKK $\beta$  (D30C6; Cell Signaling Technology, 1:2,000), phospho-p38 (Thr180/Tyr182; 28B10; Cell Signaling Technology, 1:500), p38 (Cell Signaling Technology, 1:2,000), GST (91G1; Cell Signaling Technology, 1:2,000), MyD88 (R&D Systems, AF3109, 1:500), IRAK1 (D51G7; Cell Signaling Technology, 1:2,000), TLR4 (ABclonal, A17634, 1:1,000), and mouse antisera against IL1R1 were described previously [11]. APC rat anti-mouse CD8a (BD Biosciences, 1:200); Pacific Blue™ rat anti-mouse CD4 (BD Biosciences, 1:200); PE rat anti-mouse CD4 (BD Biosciences, 1:200); PE rat anti-mouse CD25 (BD Biosciences, 1:200); APC rat anti-mouse CD45R/B220 (BD Biosciences, 1:200); FITC rat anti-mouse CD3 molecular complex (BD Biosciences, 1:500); PE anti-mouse CD49b antibody (BioLegend, 1:200); mouse IL-1 $\beta$  ELISA MAX™ Deluxe (BioLegend); LEGEND MAX™ Mouse IFN- $\beta$  ELISA Kit (BioLegend); and mouse TNF- $\alpha$  ELISA MAX™ Deluxe (BioLegend) were purchased from the indicated companies. SeV and HSV-1 were previously described [28,29].

In an attempt to detect RNF152 by immunoblotting, we tried two commercial RNF152 antibodies (Santa Cruz Biotechnology: sc-398407, Abclonal: A16608) and raised polyclonal antisera against four distinct immunogens (one recombinant human RNF152 proteins [aa: 1–187] and three peptides [FNYYSPPRRRPKLLDC, LQQMRTSQKDVRC, and C-EEQDRRGVVKSS]). We tested these antibodies with RNF152-overexpressed cell lysate and lysates of *Rnf152*<sup>+/+</sup> and *Rnf152*<sup>-/-</sup> MEFs or BMDM. No antibody could detect the overexpressed RNF152 readily or detect a specific band in the wild-type cells but not in the knockout cells.

## Cells

HEK293T cells were purchased from ATCC. Human PBMCs were purchased from ALLCELLS. HFFs provided by Prof. Min-Hua Luo (Wuhan Institute of Virology, CAS) were derived from human foreskins (male) [30]. These cells were cultured in DMEM (HyClone) supplemented with 10% fetal bovine serum (Gibco) and 1% penicillin–streptomycin (Thermo Fisher Scientific) at 37°C with 5% CO<sub>2</sub>.

## Overexpression screening

The genome-scale expression library of human ORFs was purchased from GE healthcare [31]. The overexpression plasmids (pLX304 vector, 50 ng) and pNifty-Luciferase reporter (a reporter to indicate NF- $\kappa$ B activation, which contains five NF- $\kappa$ B binding sites) were transfected together into HEK293T cells (48-well plates). Twenty-four hours later, cells were left untreated or stimulated with IL-1 $\beta$  for 10 h, and then, dual-luciferase assays were performed.

## Transfection and reporter assays

The HEK293T cells were seeded on 48-well plates and transfected the next day by standard calcium phosphate precipitation method. To normalize transfection efficiency, 10 ng of pRL-TK (Renilla luciferase) reporter plasmid was added. Luciferase assays were performed using a dual-specific luciferase assay kit (Promega).

## Constructs

Overexpression plasmids were constructed to pCMV14 or pRK vector by standard molecular clone methods. The point mutation plasmids were constructed by site-directed mutagenesis method. RNF152- $\Delta$ R (aa: 55–203) indicates the deletion of the RING finger domain, and RNF152- $\Delta$ TM (aa: 1–165) indicates the deletion of the transmembrane domain. MyD88-DD-ID (aa: 1–155), MyD88-DD (aa: 1–109), MyD88-ID-TIR (aa: 110–296), and MyD88-TIR (aa: 156–296) indicate the different truncations of MyD88. TLR4 was constructed into pMSCV without tag or into pRK with a Flag tag in its C-terminus. MD2 was constructed into pLX304 with a V5 tag in its C-terminus.

## RNA interference experiments

The siRNA duplexes targeting RNF152 were chemically synthesized by GenePharma. The siRNA duplexes were transfected into cells with PepMute siRNA transfection reagent (SignaGen Laboratories) according to the manufacturer's instructions. The sequences of each siRNA oligonucleotide are as follows: siRNF152-1#: CCAAGTTGCTG GACTGCAA, siRNF152-2#: GCATCGTGCTTCAACAACAT, siRNF152-3#: TGGTGCCGCGGTGTACCA, siRnf152 (mouse): GGCTTCTCTGT ATCACA, and negative control (NC): TTCTCCGAACGUGUCACGT.

## Mice

*Rnf152*<sup>-/-</sup> mice were kindly provided by Professor Wang Ping at Tongji University. The generation of *Rnf152*<sup>-/-</sup> mice has been described previously [19]. All animals were maintained in the animal facility of the Center for Animal Experiment of Wuhan Institute of Virology in specific pathogen-free condition. The genotyping of *Rnf152*<sup>-/-</sup> mice was performed by PCR with the following primers: forward: CAAGACCTCTGGGTCATCGG and reverse: GATGAGGACCAGCCAGAAGG. The PCR products were separated by 15% PAGE. All animal experiments were performed according to the Wuhan Institute of Virology animal care and use committee guidelines.

## Co-immunoprecipitation analysis

Transfected HEK293T cells were lysed in 1 ml of lysis buffer (20 mM Tris-HCl, pH 7.4, 150 mM NaCl, 1 mM EDTA, 1% NP-40) supplemented with protease and phosphatase inhibitors. For each immunoprecipitation, 400  $\mu$ l of cell lysate was incubated with 0.5  $\mu$ g of the indicated antibody and 30  $\mu$ l of 50% slurry of Protein G-Sepharose (GE Healthcare) at 4°C for 2 h. The Sepharose beads were then washed three times with 1 ml of lysis buffer containing 500 mM NaCl. The precipitates were resuspended with 40  $\mu$ l 2 $\times$  SDS loading buffer and boiled for 10 min. The Western blot was performed according to standard procedures.

## RNA extraction and qPCR

Total RNA was extracted using TRIzol according to the manufacturer's instructions. The cDNA was synthesized using oligo(dT) primer and M-MLV Reverse Transcriptase (Invitrogen). The cDNA was diluted 50-fold and subjected to qPCR. The expression in

different samples was normalized to GAPDH or ACTB. Gene-specific primer sequences are shown in Table 1.

### Immunofluorescence and confocal microscopy

Cells were stimulated as the indicated time before fixed with 4% paraformaldehyde. Cells were permeabilized with 0.1% Triton X-100 and blocked with 1% BSA. Cells were stained with the indicated primary antibodies and the corresponding secondary antibodies. Nuclei were stained with DAPI. Cells were observed with a Nikon confocal microscope.

### Generation of BMDMs, BMDCs, MEFs, and MLFs

Bone marrow cells were isolated from tibia and femur. For the preparation of BMDMs, the bone marrow cells were cultured in RPMI 1640 medium supplemented with 10% FBS and 10% M-CSF-containing supernatant from L929 cells for 4 days. For the preparation of BMDCs, the bone marrow cells were cultured in RPMI 1640 medium supplemented with 10% FBS and 10% GM-CSF for 6 days. MEFs were prepared from day 13.5 embryos and cultured in DMEM containing 10% FBS. Primary MLFs were isolated from *Myd88*<sup>+/+</sup> and *Myd88*<sup>-/-</sup> mice. Lungs were minced and digested in calcium and magnesium-free HBSS containing 10 µg/ml type II collagenase and 20 µg/ml DNase I for 1 h at 37°C. Cell suspensions were centrifuged for 10 min at 280 g, resuspended in DMEM/F-12 containing 10% FBS, and plated into cell culture dish. Cells were rinsed with PBS on the second day and were further cultured for 4 days.

### ELISA

Blood collected from the indicated mice was incubated for 1 h at 37°C and then incubated overnight at 4°C. The next day, the sera were collected after centrifugation for 5 min at 800 g. Diluted sera

were assessed with ELISA kits according to the manufacturer's instructions.

### Flow cytometry

Spleen and thymus were excised from the indicated mice for the preparation of single cell suspension. Single cell suspensions were fixed with 4% paraformaldehyde for 30 min and blocked with Fc block for 15 min. Subsequently, cells were washed with FACS buffer (PBS + 2% FBS) and stained with the indicated antibody for 30 min. After staining, cells were washed twice with FACS buffer before flow cytometry analysis.

### Recombinant protein purification and pull-down assay

Recombinant GST-RNF152-ΔTM was purified with Glutathione Sepharose (GE Healthcare) and eluted from beads with elution buffer (50 mM Tris-HCl, pH 8.0, 10 mM reduced glutathione). For pull-down assay, lysates of HEK293T cells transfected with the indicated plasmids or *Escherichia coli* containing His-tagged MyD88 were added to the purified recombinant protein coupled to Glutathione Sepharose and incubated for 2 h at 4°C. Subsequently, the beads were washed, boiled, and subjected to Western blot.

### Gel filtration chromatography

RAW 264.7 cells were transfected with siRNA targeting Rnf152 or negative control. Forty-eight hours later, cells were stimulated with LPS (1 µg/ml in final concentration) for 5 min. Subsequently, cells were cooled down in ice-water mixture and centrifuged for 5 min at 300 g, 4°C. Collected cells ( $1.5 \times 10^8$  cells per sample) were lysed in lysis buffer (20 mM Tris-HCl, pH 7.4, 150 mM NaCl, 1 mM EDTA, 1% NP-40, supplemented with protease and phosphatase inhibitors) and sonicated for 1 min. Lysates were centrifuged at 13,000 g, 4°C for 30 min, followed by filtering through a 0.45-µm syringe filter to

**Table 1.** The sequences of gene-specific primers.

Gene	Forward (5'–3')	Reverse (5'–3')
<i>GAPDH</i>	GAGTCAACGGATTGGTTCGT	GACAAGCTTCCCCTTCTCAG
<i>ACTB</i>	GGCCCGAGCCGGAGTAGCA	GATGGACGGGAACACGGCCC
<i>IL8</i>	GAGAGTGATTGAGAGTGACCAC	CACAACCCTCTGCACCAGTTT
<i>IL6</i>	CCTCAGCCCCCTCTGGGGTC	AAGTCCGCCCTGTAGGTGAGGTT
<i>CXCL1</i>	CTTCAGGAACAGCCACCAGT	TCCTGCATCCCCATAGTTA
<i>CXCL10</i>	GGTGAGAAGAGATGTCTGAATCC	GTCCATCCTTGAAGCACTGCA
<i>IL1B</i>	CCACAGACCTTCCAGGAGAATG	GTGCAGTTCAGTGATCGTACAGG
<i>RNF152</i>	AGATGAGGACCAGCCAGAAGGA	GAAGTGTGTGGAATGGCGATGAC
<i>Gapdh</i>	ACGGCCGCATCTTCTGTGCA	ACGGCCAAATCCGTTACACC
<i>Ifnb1</i>	TCCTGCTGTGCTTCTCCACCACA	CCTCAGCCCCCTCTGGGGTC
<i>Tnfa</i>	GGTGATCGGTCCCAAGGGATGA	TGGTTTGTACGACGTGGGCT
<i>Il6</i>	TCTGCAAGAGACTTCCATCCAGTTG	AGCCTCCGACTTGTGAAGTGGT
<i>Il1b</i>	CGGACCCCAAAGATGAAGGGCTG	AGCTGCCACAGCTTCTCCACA
<i>Cxcl10</i>	GCCGTCATTTTCTGCCTCA	CGTCCTTGCGAGAGGGATC
<i>Rnf152</i>	CGACGAAGGCCCAAGTTGTT	GGGCAATTTGGTGATGCC

clarify the lysates. The cleared lysates were subjected to gel filtration chromatography using Superdex 200 Increase 10/300 GL column and separation buffer (50 mM Tris, pH 7.4, 150 mM NaCl). Fraction collector collected 1 ml per fraction for 12 fractions after the 0.2 CV dead volume. A gel filtration standard (Bio-Rad 151-1901) was also run to calibrate the fractions.

HEK293T cells were transfected with the indicated plasmids. Twenty-four hours later, cells were collected and lysed in lysis buffer (20 mM Tris-HCl, pH 7.4, 150 mM NaCl, 1 mM EDTA, 1% NP-40, supplemented with protease and phosphatase inhibitors) and sonicated for 1 min. Then, the lysates were cleared and subjected to gel filtration as previously described.

### LPS-induced endotoxemia model

Age- and sex-matched *Rnf152*<sup>+/+</sup> or *Rnf152*<sup>-/-</sup> mice were intraperitoneally injected with LPS (10 mg/kg) and monitored every 4 h for their survival.

### Statistical analysis

For two samples, unpaired, two-tailed Student's *t*-test was used for statistical analysis and the *F*-test was performed to confirm that two populations have the same variances. The Shapiro–Wilk normality test was performed to confirm the normal distribution of all datasets. For multiple comparisons, one-way ANOVA was performed followed by a *post hoc* test. For the survival curves comparison, log-rank (Mantel–Cox) test was performed. Statistical differences were evaluated using GraphPad Prism 8 software.

### Ethics statement

Human foreskin fibroblasts were isolated from human foreskins (male). The original source of the anonymized tissues was the Zhongnan Hospital of Wuhan University (Wuhan, China). The cell isolation procedures and research plans were approved by the Institutional Review Board (IRB; WIVH31201701) according to the Guidelines for Biomedical Research Involving Human Subjects at the Wuhan Institute of Virology, Chinese Academy of Sciences.

**Expanded View** for this article is available online.

### Acknowledgements

This study was supported by grants from the Strategic Priority Research Program funded by Chinese Academy of Sciences (XDB29010302), the Youth Innovation Promotion Association CAS (No. 2017382), and the National Natural Science Foundation of China (No. 31621061). We thank Professor Ping Wang at Tongji University for kindly providing us with *Rnf152*<sup>-/-</sup> mice. We thank Xue-Fang An, He Zhao, Fan Zhang, and Li Li from the Center for Animal Experiment of Wuhan Institute of Virology for their help with animal experiments. We thank Juan Min from the Center for Instrumental Analysis and Metrology of Wuhan Institute of Virology for her help with flow cytometry.

### Author contributions

YR, M-GX, and Y-YW conceived and designed the study. YR, M-GX, Y-HL, Z-SX, and S-YW performed the experiments. YR, M-GX, and Y-YW analyzed the data. YR, M-GX, Z-SX, and Y-YW wrote the manuscript. All of the authors discussed the results and commented on the manuscript.

### Conflict of interest

The authors declare that they have no conflict of interest.

### References

- Kawai T, Akira S (2010) The role of pattern-recognition receptors in innate immunity: update on toll-like receptors. *Nat Immunol* 11: 373–384
- O'Neill LA, Golenbock D, Bowie AG (2013) The history of toll-like receptors - redefining innate immunity. *Nat Rev Immunol* 13: 453–460
- Sims JE, Smith DE (2010) The IL-1 family: regulators of immunity. *Nat Rev Immunol* 10: 89–102
- Wesche H, Henzel WJ, Shillinglaw W, Li S, Cao Z (1997) MyD88: an adapter that recruits IRAK to the IL-1 receptor complex. *Immunity* 7: 837–847
- Muzio M, Ni J, Feng P, Dixit VM (1997) IRAK (Pelle) family member IRAK-2 and MyD88 as proximal mediators of IL-1 signaling. *Science* 278: 1612
- Cao Z, Henzel WJ, Gao X (1996) IRAK: a kinase associated with the interleukin-1 receptor. *Science* 271: 1128
- Cao Z, Xiong J, Takeuchi M, Kurama T, Goeddel DV (1996) TRAF6 is a signal transducer for interleukin-1. *Nature* 383: 443
- Deng L, Wang C, Spencer E, Yang L, Braun A, You J, Slaughter C, Pickart C, Chen ZJ (2000) Activation of the I $\kappa$ B kinase complex by TRAF6 requires a dimeric ubiquitin-conjugating enzyme complex and a unique polyubiquitin chain. *Cell* 103: 351–361
- Wang C, Deng L, Hong M, Akkaraju GR, Inoue J-I, Chen ZJ (2001) TAK1 is a ubiquitin-dependent kinase of MKK and IKK. *Nature* 412: 346
- Gay NJ, Gangloff M, O'Neill LAJ (2011) What the Myddosome structure tells us about the initiation of innate immunity. *Trends Immunol* 32: 104–109
- Lin H, Gao D, Hu M-M, Zhang M, Wu X-X, Feng L, Xu W-H, Yang Q, Zhong X, Wei J *et al* (2018) MARCH3 attenuates IL-1 $\beta$ -triggered inflammation by mediating K48-linked polyubiquitination and degradation of IL-1RI. *Proc Natl Acad Sci USA* 115: 12483
- Ye W, Hu M-M, Lei C-Q, Zhou Q, Lin H, Sun M-S, Shu H-B (2017) TRIM8 negatively regulates TLR3/4-mediated innate immune response by blocking TRIF–TBK1 interaction. *J Immunol* 199: 1856
- Hu M-M, Yang Q, Zhang J, Liu S-M, Zhang Y, Lin H, Huang Z-F, Wang Y-Y, Zhang X-D, Zhong B *et al* (2014) TRIM38 inhibits TNF $\alpha$ - and IL-1 $\beta$ -triggered NF- $\kappa$ B activation by mediating lysosome-dependent degradation of TAB 2/3. *Proc Natl Acad Sci USA* 111: 1509
- Hu M-M, Xie X-Q, Yang Q, Liao C-Y, Ye W, Lin H, Shu H-B (2015) TRIM38 negatively regulates TLR3/4-mediated innate immune and inflammatory responses by two sequential and distinct mechanisms. *J Immunol* 195: 4415
- Li Q, Yan J, Mao A-P, Li C, Ran Y, Shu H-B, Wang Y-Y (2011) Tripartite motif 8 (TRIM8) modulates TNF $\alpha$ - and IL-1 $\beta$ -triggered NF- $\kappa$ B activation by targeting TAK1 for K63-linked polyubiquitination. *Proc Natl Acad Sci USA* 108: 19341
- Chen R, Li M, Zhang Y, Zhou Q, Shu H-B (2012) The E3 ubiquitin ligase MARCH8 negatively regulates IL-1 $\beta$ -induced NF- $\kappa$ B activation by targeting the IL1RAP coreceptor for ubiquitination and degradation. *Proc Natl Acad Sci USA* 109: 14128
- Yang Y, Wang S-Y, Huang Z-F, Zou H-M, Yan B-R, Luo W-W, Wang Y-Y (2016) The RNA-binding protein Mex3B is a coreceptor of toll-like receptor 3 in innate antiviral response. *Cell Res* 26: 288

18. Zhang S, Wu W, Wu Y, Zheng J, Suo T, Tang H, Tang J (2010) RNF152, a novel lysosome localized E3 ligase with pro-apoptotic activities. *Protein Cell* 1: 656–663
19. Deng L, Jiang C, Chen L, Jin J, Wei J, Zhao L, Chen M, Pan W, Xu Y, Chu H et al (2015) The ubiquitination of rag A GTPase by RNF152 negatively regulates mTORC1 activation. *Mol Cell* 58: 804–818
20. Gillen JG, Nita-Lazar A (2017) Composition of the myddosome during the innate immune response. *J Immunol* 198: 75.15
21. Nagpal K, Plantinga TS, Sirois CM, Monks BG, Latz E, Netea MG, Golencbock DT (2011) Natural loss-of-function mutation of myeloid differentiation protein 88 disrupts its ability to form Myddosomes. *J Biol Chem* 286: 11875–11882
22. Motshwene PG, Moncrieffe MC, Grossmann JG, Kao C, Ayaluru M, Sandercock AM, Robinson CV, Latz E, Gay NJ (2009) An oligomeric signaling platform formed by the toll-like receptor signal transducers MyD88 and IRAK-4. *J Biol Chem* 284: 25404–25411
23. George J, Motshwene PG, Wang H, Kubarenko AV, Rautanen A, Mills TC, Hill AV, Gay NJ, Weber AN (2011) Two human MYD88 variants, S34Y and R98C, interfere with MyD88-IRAK4-myddosome assembly. *J Biol Chem* 286: 1341–1353
24. Avbelj M, Wolz OO, Fekonja O, Bencina M, Repic M, Mavri J, Kruger J, Scharfe C, Delmiro Garcia M, Panter G et al (2014) Activation of lymphoma-associated MyD88 mutations via allosterically-induced TIR-domain oligomerization. *Blood* 124: 3896–3904
25. Lin SC, Lo YC, Wu H (2010) Helical assembly in the MyD88-IRAK4-IRAK2 complex in TLR/IL-1R signalling. *Nature* 465: 885–890
26. Phelan JD, Young RM, Webster DE, Roulland S, Wright GW, Kasbekar M, Shaffer AL 3rd, Ceribelli M, Wang JQ, Schmitz R et al (2018) A multiprotein supercomplex controlling oncogenic signalling in lymphoma. *Nature* 560: 387–391
27. Burns K, Martinon F, Esslinger C, Pahl H, Schneider P, Bodmer JL, Di Marco F, French L, Tschopp J (1998) MyD88, an adapter protein involved in interleukin-1 signaling. *J Biol Chem* 273: 12203–12209
28. Huang ZF, Zou HM, Liao BW, Zhang HY, Yang Y, Fu YZ, Wang SY, Luo MH, Wang YY (2018) Human cytomegalovirus protein UL31 inhibits DNA sensing of cGAS to mediate immune evasion. *Cell Host Microbe* 24: 69–80.e4
29. Ran Y, Zhang J, Liu LL, Pan ZY, Nie Y, Zhang HY, Wang YY (2016) Autoubiquitination of TRIM26 links TBK1 to NEMO in RLR-mediated innate antiviral immune response. *J Mol Cell Biol* 8: 31–43
30. Duan YL, Ye HQ, Zavala AG, Yang CQ, Miao LF, Fu BS, Seo KS, Davrinche C, Luo MH, Fortunato EA (2014) Maintenance of large numbers of virus genomes in human cytomegalovirus-infected T98G glioblastoma cells. *J Virol* 88: 3861–3873
31. Yang X, Boehm JS, Yang X, Salehi-Ashtiani K, Hao T, Shen Y, Lubonja R, Thomas SR, Alkan O, Bhimdi T et al (2011) A public genome-scale lentiviral expression library of human ORFs. *Nat Methods* 8: 659–661